Combination of point and extended target based interferometric techniques

Andreas Wiesmann, Charles Werner, Tazio Strozzi, and Urs Wegmüller
Gamma Remote Sensing, Thunstrasse 130, CH-3074 Muri, Switzerland
http://www.gamma-rs.ch, e-mail: wiesmann@gamma-rs.ch

***Abstract*— The objective of this paper is to present an approach that combines the interferometric point target analysis (IPTA) and the extended target based interferometric techniques (InSAR). The improvements achieved are most obvious in cases where the individual techniques result in complementary coverage in the information retrieved.**

Keywords: Interferometric Point Target Analysis, IPTA, InSAR, Interferometry, JERS, Surface deformation

I. Introduction

Land surface deformation monitoring with SAR interferometry has reached operational status. It is widely applied in the context of various applications using data from various sensors. Temporal and geometric decorrelation of the signal of extended targets is probably the most stringent limitation of SAR interferometry.

In recent years alternative techniques which explore the interferometric signatures of scatterers with point-like scatter characteristics have been developed. Important advantages of interferometric point target analysis (IPTA) are its potential to find scatterers in low-coherence areas and that interferometric image pairs with large baselines may be included in the analysis. Finding usable points in low-coherence regions fills spatial gaps in the deformation maps while the ability to use large baselines improves the temporal sampling. Nevertheless, the dependence on point-like scatterers is also a limitation as it restricts the applicability more or less to areas that include infrastructure.

Due to the complementarity of the two approaches, the best use of the data is achieved through a combination of both the point and extended target based interferometric techniques.

II. Test Site and Data Selection

The oil field in Belridge California [1] was selected as test area (Figure 1). A set of 5 JERS-1 scenes was available (Table 1) to monitor the ground surface deformation for the period September 1994 to August 1996.

III. Data Processing

The 2-pass approach [2] was used to derive the differential interferograms indicated in Table I. For pairs with a perpendicular baseline component below 2 km the coherence was found to be high enough for interpretation of the phase for the area of the oil fields. Apart from water surfaces very low correlation was mainly observed for specific agricultural fields as a consequence of cultivation. The differential interferograms were unwrapped, using a minimum cost flow optimisation technique [3]. The initial baseline estimates derived from the orbit data were improved using a least-squares optimisation with height control points extracted from a USGS DEM, leading to quite significant changes (see Table I). For long baselines above 3500m, and therefore very low coherence this approach was not applicable. Using the improved baselines the interferograms

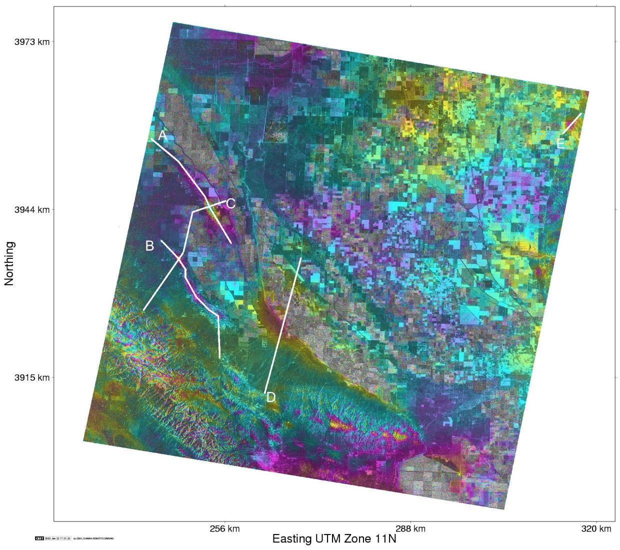

Figure 1. Orthorectified differential interferogram (940909_950119) over Belridge, California. One color cycle corresponds to 2π interferometric phase. The image is using the USGS DEM and in UTM zone 11N projection.

TABLE I. INTERFEROMETRIC PAIRS OF JERS-1 DATA AND CORRESPONDING BASELINES.

Pair	Elapsed time [days]	Base perp. (orbit) [m]	Base perp. Improved [m]
940909_950119	132	-607.9	-611.6
940909_950417	220	634.2	548.7
940909_960403	572	1142.3	971.6
940909_960813	704	3205.2	2970.0
950119_950417	88	1241.6	1160.2
950119_960403	440	1749.3	1583.1
950119_960813	572	3810.9	NA
950417_960403	352	508.6	423.4
950417_960813	484	2572.6	2483.8
960403_960813	132	2064.8	2054.0

were computed (Figure 2). For the same area scatterers with point-like scatter characteristics were identified and their differential interferometric phases were calculated using the identical height reference and phase model. The 2d differential interferometric phases and the corresponding point target based differential interferometric phases were now combined and spatially unwrapped (Figures 3 to 5). Finally, the unwrapped phases were converted to vertical deformation values (Figures 6 to 8).

IV. RESULTS

The differential interferogram that covers the full 704 days is shown in Figure 2. Due to the large baseline of almost 3km (Table 1) and the temporal decorrelation the coherence is quite low, so that the phases could not be unwrapped for large areas. In [1] we have shown the potential of 2d differential InSAR with the same dataset for the same test site. It turned out that the deformation over the full observation time could only be retrieved from combinations of shorter periods with small baselines.

Many point like scatterers could be identified, including points in areas of low coherence in all 2D differential interferograms, and points in areas of low coherence in some 2D differential interferograms. Considering the small available data stack and the high deformation rates spatial phase unwrapping of the point phases was required. This turned out to be very difficult, though, because of the strong terrain deformation.

In the combination we identified important contributions by both techniques that are synergetic. IPTA contributed additional points, it also contributed points that can be interpreted in all interferogram pairs which is important for building time series. In the case of pairs with relatively short baselines and time intervals the 2D interferometry provided better information for spatial unwrapping. It also improved the spatial coverage and the spatial resolution for the subsidence cones. Therefore, the synergistic use of both techniques permitted to improve the result achieved.

In Figures 3 to 5 the unwrapped differential interferograms for selected pairs are shown. Figure 3 shows the unwrapped phase based on IPTA and 2D differential interferometry between 9.9.94 and 17.4.95. The corresponding baseline is 1.2 km. The active areas are well covered. The corresponding vertical displacements are shown in Figure 6. The maximum subsidence is 30cm in 220 days. Figure 4 shows the unwrapped phase based on IPTA and 2D differential interferometry between 9.9.94 and 3.4.96. The corresponding baseline is 1.7 km. Again the active areas are well covered. The unwrapped area is increased as compared to [1] and the vertical displacement was directly computed from this 573 day unwrapped interferogram (Figure 7). In [1] the combination of 940909 with 950417 and 950417 with 960403 was used to derive the total displacement for this 573 day period. The maximum total deformation observed was 75 cm. In Figure 5 the unwrapped phase based on IPTA and 2D differential interferometry between 9.9.94 and 13.8.96 is shown. The corresponding baseline is 3 km. Comparing with Figure 2 that shows the 2D differential interferogram over the same period, the benefit of the combination of 2D InSAR with IPTA is impressive. While in [1] we had to combine 940909_950417, 950417_960403, and 960403_960813 to retrieve the total deformation over 704 days, here we retrieved the total vertical displacement directly from one unwrapped interferogram at an even better spatial coverage. With the direct displacement calculation we avoid the adding of errors when we add displacements from several pairs.

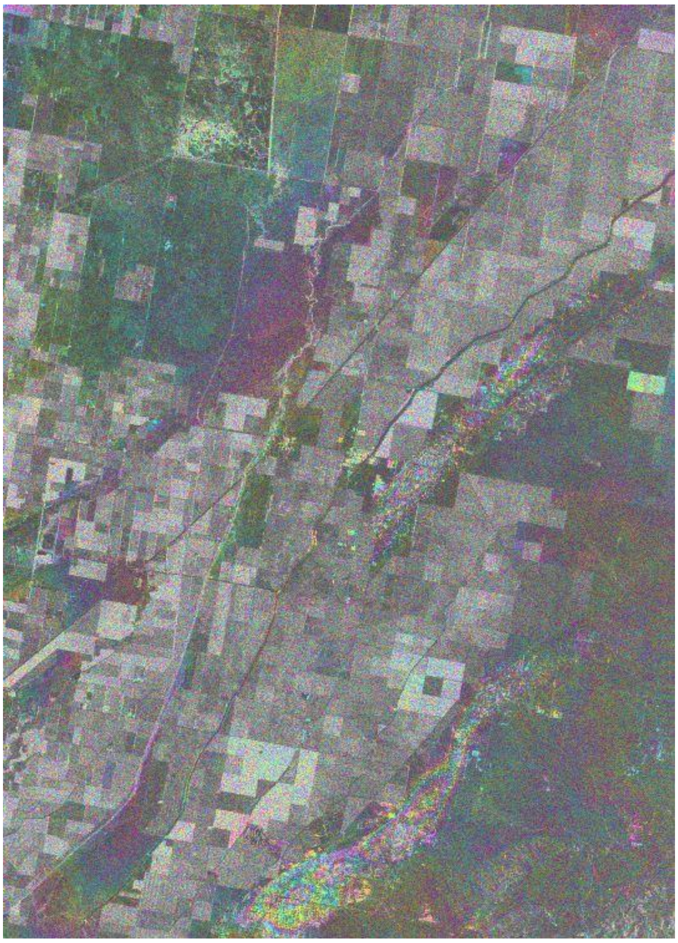

Figure 2. Differential interferogram between 9.9.94 and 13.8.96 (704 days, perpendicular baseline 2970m).

V. CONCLUSIONS

In the present study the good potential of combining point and extended target based interferometry techniques was demonstrated. The synergetic combination of the strengths of the two complementary techniques permitted to achieve a better overall result. An important observation is the complementary spatial coverage. Specific IPTA strengths include additional points in low coherence areas, points which can be interpreted in all pairs (even with large baselines), with related advantages for the building of time series. Particular 2D interferometry strengths include advantages in the coverage and spatial sampling in some areas. In the case of the Belridge example the 2D interferometry supported the phase unwrapping for the subsidence cones.

REFERENCES

[1] Wiesmann A., U. Wegmüller, C. Werner and T.Strozzi, Subsidence monitoring over oil fields with L-band SAR interferometry, IGARSS'03, Toilouse France, 21-25 July, 2003.

[2] Wegmüller U., and T. Strozzi, Characterization of differential interferometry approaches, EUSAR'98, 25-27 May, Friedrichshafen, Germany, VDE-Verlag, ISBN 3-8007-2359-X, pp. 237-240, 1998.

[3] Werner C., U. Wegmüller, and T. Strozzi, Processing strategies for phase unwrapping for INSAR applications, Procs. EUSAR Conf., Cologne, Germany, 4.-6. June, 2002.

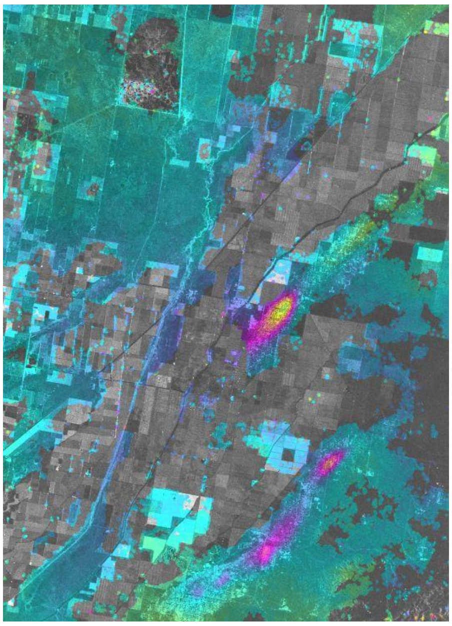

Figure 3. Unwrapped phase based on IPTA and 2D differential interferometry between 9.9.94 and 17.4.95 of the Lost Hills – Belridge area. A color cycle corresponds to about 10 cm deformation in the line of sight.

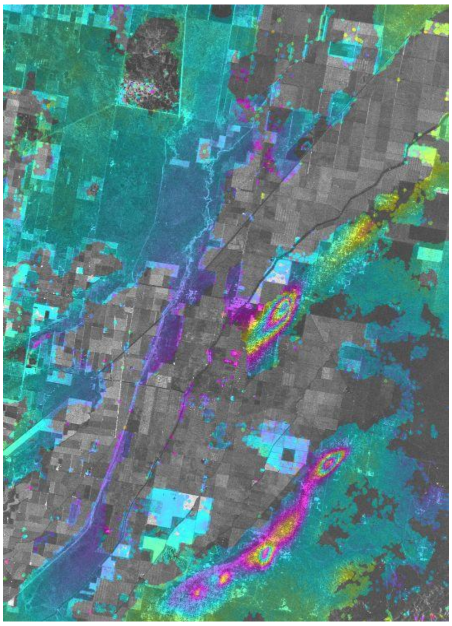

Figure 4. Unwrapped phase based on IPTA and 2D differential interferometry between 9.9.94 and 3.4.96 of the Lost Hills – Belridge area. A color cycle corresponds to about 10 cm deformation in the line of sight.

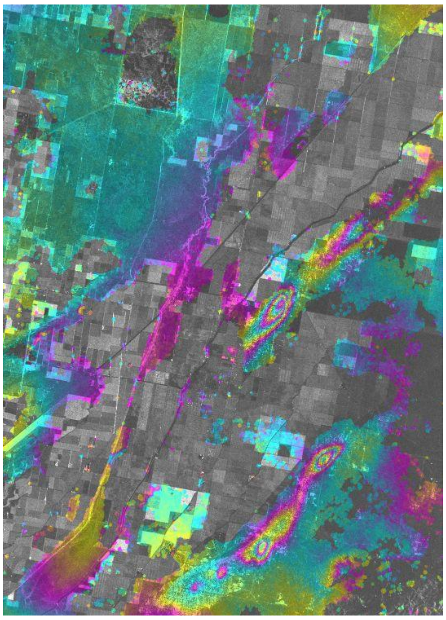

Figure 5. Unwrapped phase based on IPTA and 2D differential interferometry between 9.9.94 and 13.8.96 of the Lost Hills – Belridge area. A color cycle corresponds to about 10 cm deformation in the line of sight.

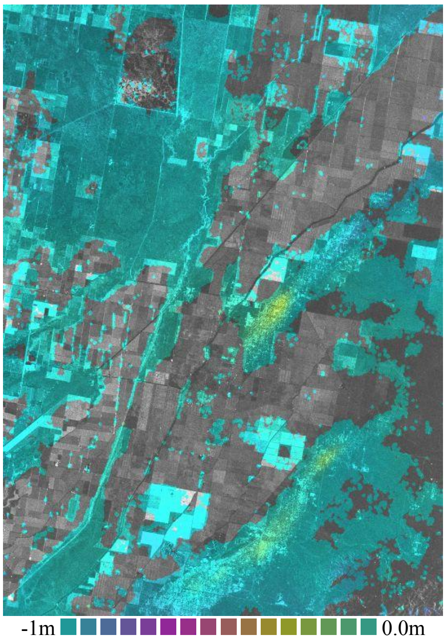

Figure 6. Vertical displacement at the Lost Hills – Belridge area based on IPTA and 2D differential interferometry for the period 9.9.94 – 17.4.95.

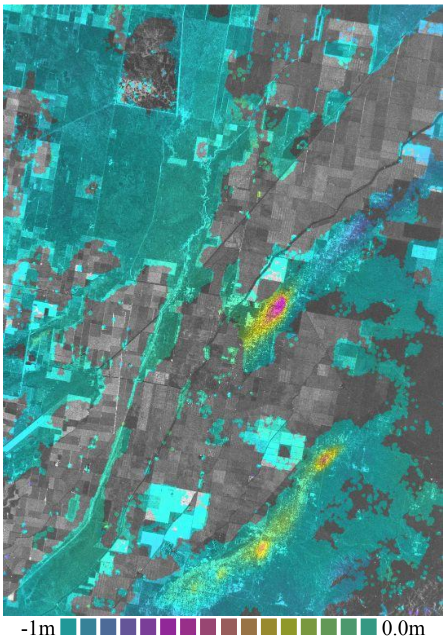

Figure 7. Vertical displacement at the Lost Hills – Belridge area based on IPTA and 2D differential interferometry for the period 9.9.94 – 3.4.96.

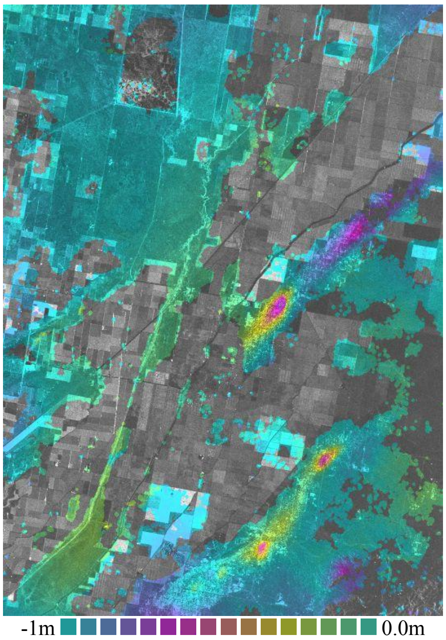

Figure 8. Vertical displacement at the Lost Hills – Belridge area based on IPTA and 2D differential interferometry for the period 9.9.94 – 13.8.96.